HUMAN GENE THERAPY 21:993–1004 (August 2010)

DOI: 10.1089/hum.2009.218

Replacement Gene Therapy with a Human *RPGRIP1* Sequence Slows Photoreceptor Degeneration in a Murine Model of Leber Congenital Amaurosis

Basil S. Pawlyk,[1] Oleg V. Bulgakov,[1,3] Xiaoqing Liu,[1] Xiaoyun Xu,[1] Michael Adamian,[1] Xun Sun,[1,3] Shahrokh C. Khani,[2] Eliot L. Berson,[1] Michael A. Sandberg,[1] and Tiansen Li[1,3]

Abstract

RPGR-interacting protein-1 (RPGRIP1) is localized in the photoreceptor-connecting cilium, where it anchors the RPGR (retinitis pigmentosa GTPase regulator) protein, and its function is essential for photoreceptor maintenance. Genetic defect in *RPGRIP1* is a known cause of Leber congenital amaurosis (LCA), a severe, early-onset form of retinal degeneration. We evaluated the efficacy of replacement gene therapy in a murine model of LCA carrying a targeted disruption of *RPGRIP1*. The replacement construct, packaged in an adeno-associated virus serotype 8 (AAV8) vector, used a rhodopsin kinase gene promoter to drive *RPGRIP1* expression. Both promoter and transgene were of human origin. After subretinal delivery of the replacement gene in the mutant mice, human RPGRIP1 was expressed specifically in photoreceptors, localized correctly in the connecting cilia, and restored the normal localization of RPGR. Electroretinogram and histological examinations showed better preservation of rod and cone photoreceptor function and improved photoreceptor survival in the treated eyes. This study demonstrates the efficacy of human gene replacement therapy and validates a gene therapy design for future clinical trials in patients afflicted with this condition. Our results also have therapeutic implications for other forms of retinal degenerations attributable to a ciliary defect.

Introduction

Retinitis pigmentosa (RP) has a prevalence of about 1 in 4000, affecting more than 1 million individuals worldwide (Berson, 1993). Patients with RP typically develop symptoms of night blindness during early adulthood followed by progressive loss of visual field and eventual blindness by 50–60 years of age (Berson, 1993). LCA is a more severe form of retinal degeneration with visual deficit in early childhood and loss of vision by the second and third decades of life (Heher *et al.*, 1992; Fulton *et al.*, 1996; den Hollander *et al.*, 2008). Clinical findings indicate that both rod and cone photoreceptors are affected early in LCA patients. Mutations in at least 15 different genes are known to cause LCA (Koenekoop, 2004; den Hollander *et al.*, 2008; Wang *et al.*, 2009), one of which is the gene encoding the RPGRIP1 protein (Dryja *et al.*, 2001; Gerber *et al.*, 2001; Koenekoop, 2005). About 6% of all cases of LCA are caused by mutations in *RPGRIP1* (Dryja *et al.*, 2001; Gerber *et al.*, 2001; den Hollander *et al.*, 2008).

RPGRIP1 was initially discovered through protein interaction screens using RPGR as bait (Boylan and Wright, 2000; Roepman *et al.*, 2000; Hong *et al.*, 2001). RPGR is also an essential protein in photoreceptors and defects in RPGR underlie the most common form of X-linked RP (Vervoort *et al.*, 2000). RPGRIP1 is normally localized to the photoreceptor connecting cilium, a thin bridge that links the inner and outer segment of the photoreceptor cell (Hong *et al.*, 2001). It appears to be a stable component of the ciliary axoneme (Hong *et al.*, 2001). We previously generated a line of mutant mice lacking RPGIRIP1 through targeted disruption of the *RPGRIP1* gene. We showed that one of its key functions was to anchor RPGR in the connecting cilia (Zhao *et al.*, 2003). In *RPGRIP1*$^{-/-}$ mice, RPGR is mislocalized and no longer found at the connecting cilium. Thus, loss of RPGRIP1 would appear to encompass the loss of RPGR function as well. RPGRIP1 also performs additional function(s) at the connecting cilium, because mice lacking RPGRIP1 have a much more severe retinal phenotype than mice lacking RPGR alone. *RGRPIP1* mutant

[1]Berman-Gund Laboratory for the Study of Retinal Degenerations, Harvard Medical School, and Massachusetts Eye and Ear Infirmary, Boston, MA 02114.
[2]Schepens Eye Research Institute, Harvard Medical School, Boston, MA 02114.
[3]Present address: Neurobiology, Neurodegeneration, and Repair Laboratory, National Eye Institute, Bethesda, MD 20892.

photoreceptors exhibit profound disruption of the outer segment structure and mislocalization of opsin proteins in rods and cones. We have hypothesized that RPGRIP1 may be involved in photoreceptor disc morphogenesis. Photoreceptors are nearly completely lost by about 5 months of age in the *RPGRIP1* mutant mice (Pawlyk *et al.*, 2005). This relatively fast rate of photoreceptor degeneration in the *RPGRIP1*$^{-/-}$ mutant makes it a useful model of LCA both for studying the disease mechanism and for testing new therapies.

At present there is no effective treatment for LCA. Gene replacement therapy using delivery vectors derived from adeno-associated virus (AAV) has emerged as a promising potential therapy for retinal degeneration. Proof-of-principle experiments in animal models have been conducted for several forms of LCA, with various degrees of success (Flannery *et al.*, 1997; Acland *et al.*, 2001; Narfstrom *et al.*, 2003; Dejneka *et al.*, 2004; Pawlyk *et al.*, 2005; Pang *et al.*, 2006; Tan *et al.*, 2009; Sun *et al.*, 2010). Phase I gene therapy trials in patients with LCA, targeting RPE65 gene defects in RPE cells, have been conducted. These clinical trials have yielded important preliminary outcomes indicating that this approach could be effective in restoring some degree of visual function (Bainbridge *et al.*, 2008; Hauswirth *et al.*, 2008; Maguire *et al.*, 2008). Clinical trials targeting photoreceptor-specific gene defects, such as *RPGRIP1* mutations, have not yet been initiated. We previously investigated AAV-mediated gene therapy in the *RPGRIP1*$^{-/-}$ mouse, using a murine-derived *RPGRIP1* replacement gene in combination with a rhodopsin gene promoter that drove expression primarily in rods (Pawlyk *et al.*, 2005), and found substantial rescue of rod photoreceptor structure and function. Although that study provides proof that gene replacement is an effective approach to restoring photoreceptor viability due to loss of RPGRIP1 function, the vector design does not readily translate into clinical studies because the replacement gene was of mouse origin and its expression was limited to rods. In the present study, we attempted to rescue the *RPGRIP1*$^{-/-}$ mouse retinal phenotype by using a short promoter derived from the rhodopsin kinase (RK) gene, which has been shown to drive cell-specific expression in rods and cones (Young *et al.*, 2003; Khani *et al.*, 2007; Sun *et al.*, 2010). Both the promoter and the *RPGRIP1* replacement gene used in the present study were of human origin. We designed the present study so that, if successful, the data and the vector design may serve as the framework for future clinical trials in patients with LCA due to *RPGRIP1* mutations.

Materials and Methods

Animals

The generation and analysis of *RPGRIP* $^{-/-}$ mice have been described previously (Zhao *et al.*, 2003). The *RPGRIP1*$^{-/-}$ mice used in this study were bred from the colony maintained in our institutional animal facility. Wild-type (WT) mice used in the study were C57BL from Charles River Laboratory (Wilmington, MA). Mice were maintained under a 12-hr light/12-hr dark lighting cycle.

Plasmid constructions and production of recombinant AAV2/8

A plasmid clone carrying the full-length human RPGRIP1 cDNA was obtained from Origene (cat. no. SC304750) (GenBank access no. NM_020366). The coding region of the human RPGRIP1 cDNA (3861 bp) was excised from the vector and inserted into our pAAV-RK-IZsGeen cloning vector between *Not*I and *Xho*I restriction sites. The resulting pAAV-RK-hRPGRIP1 construct was packaged into AAV2/8 pseudotyped vector by tripartite transfection (AAV vector plasmid encoding the gene of interest, AAV helper plasmid pLT-RC03 encoding AAV Rep proteins from serotype 2 and Cap proteins from serotype 8, and adenovirus helper miniplasmid pHGTI-Adeno1) into 293A cells. The transfection was performed according to a published protocol (Xiao *et al.*, 1998). Two days after transfection, cells were lysed by repeated freeze and thaw cycles. After initial clearing of cell debris, the nucleic acid component of the virus producer cells was removed by Benzonase treatment. The recombinant AAV vector particles were purified by iodixanol density gradient. The purified vector particles were dialyzed extensively against phosphate-buffered saline (PBS) and titered by dot-blot hybridization. As a control vector, enhanced green fluorescent protein (EGFP) replaced the RPGRIP1 cDNA.

Subretinal injection

Mice were placed under general anesthesia with an intraperitoneal injection of ketamine (90 mg/kg)–xylazine (9 mg/kg). A 0.5% proparacaine solution was applied to the cornea as a topical anesthetic. Pupils were dilated with topical application of cyclopentolate hydrochloride and phenylephrine hydrochloride. Under an ophthalmic surgical microscope, a small incision was made through the cornea adjacent to the limbus, using an 18-gauge needle. A 33-gauge blunt needle fitted to a Hamilton syringe was inserted through the incision while avoiding the lens and pushed through the retina. All injections were made subretinally in a location within the nasal quadrant of the retina. Each animal received 0.5–1 μl of AAV at 1×10^{12} particles/ml. Treatment vector was typically given in the left eye (OS) and control vector was given in the fellow eye (OD), and they are referred to throughout this text as "treated" and "control," respectively. Cohorts of mice ($n = 50$) were injected at approximately postnatal day 14.

Histology and immunofluorescence

For both light microscopy and transmission electron microscopy, enucleated eyes were fixed for 10 min in 1% formaldehyde, 2.5% glutaraldehyde in 0.1 *M* sodium cacodylate buffer (pH7.5). After removal of the anterior segments and lens, the eye cups were left in the same fixative at 4°C overnight. Eye cups were washed with buffer, postfixed in 2% osmium tetroxide, dehydrated through a graded alcohol series, and embedded in Epon. Semithin sections (1 μm) were cut for light microscopic observations. For electron microscopy, ultrathin sections (70 nm) were stained with uranyl acetate and lead citrate before viewing on a JEOL 100CX electron microscope. For morphometric analyses of photoreceptor inner and outer segment (IS/OS) length and outer nuclear layer (ONL) thickness, measurements were made along the vertical meridian at three locations to each side of the optic nerve head separated by about 500 μm each. Measurements began at about 500 μm from the optic nerve head itself.

For immunofluorescence, eyes were enucleated and placed in fixative, and their anterior segment and lens were

removed. The fixative was composed of 2% formaldehyde, 0.25% glutaraldehyde in PBS. The duration of fixation was typically 20 min. The fixed tissues were soaked in 30% sucrose–PBS for at least 2 hr, shock frozen, and sectioned at 10-μm thickness in a cryostat. Sections were collected into PBS buffer and remained free-floating for the duration of the immunostaining process. In some cases, eyes were unfixed and frozen sections were collected on glass slides. Sections were viewed and photographed on a laser scanning confocal microscope (model TCS SP2; Leica).

Antibodies used were anti-mouse RPGRIP1, anti-human RPGRIP1, anti-mouse RPGR (S1), anti-rootletin, anti-rhodopsin (rho 1D4; gift from R. Molday) (Molday, 1988), green cone anti-opsin, and Hoechst 33342 (a nuclear dye stain). Rabbit anti-human RPGRIP1 was generated by Cocalico Biologicals (Reamstown, PA), using amino acids 964–1274 from human RPGRIP1. Antigen was amplified by PCR, using the Origene clone as a template, and primers (sense: hRPGRIP-1S, GGAATTCCCCAGGATCAGATGGCATCTCC; antisense: hRPGRIP-1R, CCCAAGCTTGCATGGAGGACAG CAGCTGC). The PCR product was inserted into the pET-28 vector between the *Eco*RI and *Hin*dIII sites, expressed in BL21, Codon+ cells (Stratagene, La Jolla, CA), and purified by passage through a histidine tag (His-tag)-binding column.

Electroretinogram recording

Methods for recording dark- and light-adapted electroretinograms (ERGs) have been previously described (Sun *et al.*, 2010). Briefly, mice were dark-adapted overnight and anesthetized, and had both pupils dilated. Rod-dominated responses were elicited in the dark with 10-μsec flashes of white light (1.37×10^5 cd/m^2) presented at intervals of 1 min in a Ganzfeld dome. Light-adapted, cone responses were elicited in the presence of a 41-cd/m^2 rod-desensitizing white background with the same flashes (1.37×10^5 cd/m^2) presented at 1 Hz. ERGs were monitored simultaneously from both eyes, with signal averaging for cone responses.

Statistical analysis

JMP, version 6 (SAS Institute, Cary, NC) was used to compare outcomes in treated versus control eyes by the one-tailed paired *t* test. For these interocular comparisons, non-detectable dark-adapted (single flash) amplitudes were coded as 5 μV and nondetectable light-adapted (averaged) amplitudes were coded as 2 μV. To evaluate the effects of treatment on loss of ERG function (which are summarized in Table 1), amplitudes were first converted to the log scale because ERG amplitude declines in animal and human retinal degenerations have been found to follow an exponential course (Clarke *et al.*, 2000; Berson *et al.*, 2002). We then used repeated measures longitudinal regression with PROC MIXED of SAS, version 9.1 to quantify rates of decline of the ERG rod a-wave, rod b-wave, and cone b-wave in treated and control eyes and to determine whether differences between treated and control eyes were significant. We used all available data for these analyses, including data from mice with missing time points, when data from both treated and fellow control eyes were available.

Results

AAV-mediated expression of human RPGRIP1 in mouse retina

The entire coding region of human RPGRIP1 cDNA was inserted downstream from the human RK promoter and an SV40 splice donor/splice acceptor element (SV40 SD/SA). The hRGPGRIP1 cDNA was terminated at the 3′ end by a polyadenylation signal (Fig. 1A, wtpA + MZ). The completed replacement gene construct (Fig. 1A) was packaged into an AAV2/8 vector (treatment vector). Treatment and control vectors were injected subretinally into cohorts of *RPGRIP1*$^{-/-}$ mice at 2 weeks of age, with each animal receiving the treatment vector in one eye and the control vector in the fellow eye. At 2 to 3 weeks after subretinal delivery, a group of mice were killed and their retinas analyzed by immunoblotting and by immunofluorescence for RPGRIP1 expression. A single band migrating at about 170 kDa was found in the treated but not control retinas by immunoblotting that matched precisely the endogenous RPGRIP1 protein from human donor retinas (Fig. 1B). This observation provided assurance that the human *RPGRIP1* cDNA sequence in the replacement gene construct corresponded to the predominant form of *RPGRIP1* transcript in human photoreceptor cells. The endogenous mouse RPGRIP1 (WT) had a higher apparent molecular mass than that of human RPGRIP1, which is consistent with molecular mass predictions based on sequences (UniProtKB accession no. Q9EPQ2 and Q96KN7 for human and mouse RPGRIP1, respectively). It appeared that the expression level of human RPGRIP1 protein was less in the treated retinas as compared with that expressed endogenously in WT mice (see Discussion).

Human RPGRIP1 expression from the treatment vector was further confirmed by immunofluorescence (Fig. 2). Endogenous mouse RPGRIP1 is normally localized in the

Table 1. Rates of Change in ERG Amplitudes in Control and Treated Eyes[a]

Component	n	*Control eye* ($\log_e$ unit/mo.)	p *Value*	*Treated eye* ($\log_e$ unit/mo.)	p *Value*	p *Value OD-OS*
Rod a-wave	37	–0.47 ± 0.03 (–37%)[b]	<0.0001	–0.08 ± 0.02 (–8%)	0.0002	<0.0001
Rod b-wave	37	–0.25 ± 0.03 (–22%)	<0.0001	–0.08 ± 0.03 (–8%)	0.0038	<0.0001
Cone b-wave	16	–0.29 ± 0.11 (–25%)	0.0212	0.20 ± 0.13	0.14	0.0026

[a]Table 1 lists the mean $\log_e$ monthly rates of change and corresponding levels of significance by ERG component for control and treated eyes, based on mice tested between 2 and 5 months of age. The last column gives the levels of significance for the difference in the rates for control (OD) and treated (OS) fellow eyes. The mean rates of decline without treatment ranged from 22%/month for the rod b-wave to 37%/month for the rod a-wave and, with treatment, these rates of decline fell to 8% for the rod a-wave and rod b-wave and to no detectable change for the cone b-wave—in each case a significant slowing of disease course.

[b]Parentheses include percent monthly rates of change for significant effects.

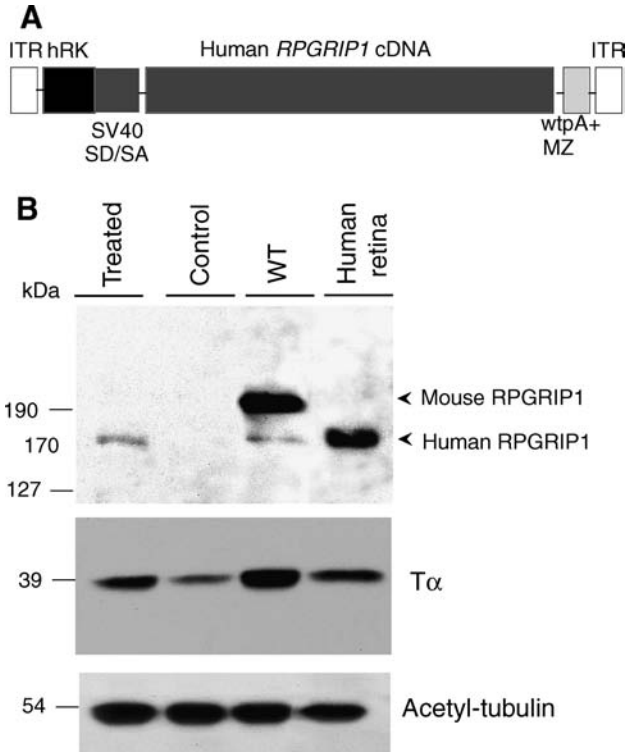

FIG. 1. Design of the treatment vector and confirmation of transgene expression. (**A**) Schematic diagram of the replacement gene construct in which the human RPGRIP1 cDNA was placed under the control of a human rhodopsin kinase (RK) promoter (AAV-RK-hRPGRIP1). The RK promoter is approximately 200 bp in length and the hRPGRIP1 cDNA is approximately 4 kb. ITR, inverted terminal repeat; hRK, RK promoter; SV40SD/SA, splice donor/acceptor sequences derived from the SV40 virus; wtpA + MZ, polyadenylation signal. This construct was packaged into an AAV vector (treatment vector). As control, a vector carrying the EGFP reporter in place of hRPGRIP1 was used (control vector). (**B**) Immunoblotting analysis with an anti-human RPGRIP1 antibody for expression from the therapeutic vector after subretinal injection of AAV vectors. Subretinal delivery of the treatment vector led to a 170-kDa protein in the *RPGRIP1*$^{-/-}$ mouse retina (Treated). This band comigrated with the RPGRIP1 protein from human retina (Human retina), indicating that the human *RPGRIP1* coding cDNA used in constructing the therapeutic vector was the correct one. This 170-kDa band was not seen in the *RPGRIP1*$^{-/-}$ mouse fellow eye that had received the control vector subretinally (Control). The major mouse RPGRIP1 protein had a substantially higher molecular mass and migrated at about 190 kDa (WT; uninjected). A much fainter band at a lower molecular mass in the uninjected WT retina may be a minor RPGRIP1 variant or a degradation product of the major mouse RPGRIP1 protein. A transducin α subunit (Tα; photoreceptor specific) and α-acetylated tubulin (expressed throughout the retina) were probed as loading controls.

photoreceptor connecting cilia (Fig. 2A, left). Antibody staining against rootletin, the structural constituent of the ciliary rootlet, served as a reference marker (J. Yang *et al.*, 2002). The ciliary rootlet extends proximally from the connecting cilium, separated only by a basal body (J. Yang *et al.*, 2002), such that the connecting cilium sits atop the rootlet in the images (Fig. 2). In *RPGRIP1*$^{-/-}$ mouse retinas receiving the control vector, RPGRIP1 was absent, whereas RPGRIP1 was found at the connecting cilia in treated retinas (Fig. 2A, middle and right). These data show that the recombinant human RPGRIP1 expressed from the treatment vector was able to localize to the correct subcellular compartment. Because one of the well-defined functions of RPGRIP1 is to anchor RPGR in the connecting cilia, we examined whether human RPGRIP1 was able to do so in mouse photoreceptors. By immunofluorescence, mouse RPGR was found at the connecting cilia in a WT mouse retina (Fig. 2B, left). In *RPGRIP1*$^{-/-}$ retinas receiving the control vector, there was no mouse RPGR signal at the cilia (Fig. 2B, middle). On delivery of the treatment vector, however, the normal localization of endogenous mouse RPGR in the cilia was restored (Fig. 2B, right). Thus human RPGRIP1 localized correctly in mouse photoreceptors and anchored mouse RPGR to the connecting cilia.

Treatment with human RPGRIP1 replacement gene preserves photoreceptor function

To evaluate the efficacy of the treatment, retinal function was measured by ERG in cohorts of *RPGRIP1*$^{-/-}$ mice at various ages after subretinal injection of the treatment vector in one eye (OS) and control vector in the fellow eye (OD) at postnatal day 14. Simultaneous bilateral recordings were performed to optimize comparison of the treated and control eyes. Dark- and light-adapted ERGs were recorded to evaluate responses from rod and cone systems, respectively. Rod ERGs were recorded at 2, 3, and 5 months of age. At 2 months, the treated eye in the vast majority of mice had larger rod ERG a-wave and b-wave amplitudes than the fellow control eye (Fig. 3A). As a group, the geometric mean values for rod ERG a-wave and b-wave amplitudes were significantly higher in the treated eyes than in the control eyes. Rod a-wave amplitudes averaged 58 μV for the treated eyes and 37 μV for the control eyes ($p = 0.0002$), and b-wave amplitudes averaged 300 μV for the treated eyes and 205 μV for the control eyes ($p = 0.0001$). At the 3-month time point (Fig. 3B), the treatment effect on retinal function was more evident. Geometric mean values for rod ERG a-wave amplitudes averaged 43 and 20 μV for the treated and control eyes, respectively ($p < 0.0001$). Geometric mean values for rod ERG b-wave amplitudes averaged 250 and 160 μV for the treated and control eyes, respectively ($p < 0.0001$). Notably, some mice with a lower ERG amplitude in their treated eye than in their control eye at 2 months showed amplitude reversal between eyes at 3 months. By 5 months of age, the difference between control and treated eyes for rod ERG amplitudes was even more pronounced (Fig. 3C). Geometric mean values for rod ERG a-wave amplitudes averaged 48 and 15 μV for the treated and control eyes, respectively ($p < 0.0001$). Geometric mean values for rod ERG b-wave amplitudes averaged 300 and 100 μV for the treated and control eyes, respectively ($p < 0.0001$).

A beneficial effect of treatment was also seen for cone function. We recorded cone ERGs at 3 and 5 months of age (Fig. 3B and C). At 3 months of age, cone ERG amplitudes were significantly higher in the treated eyes than in the control eyes, with geometric mean cone ERG b-wave amplitudes being 13 and 5 μV, respectively ($p < 0.001$). At 5 months of

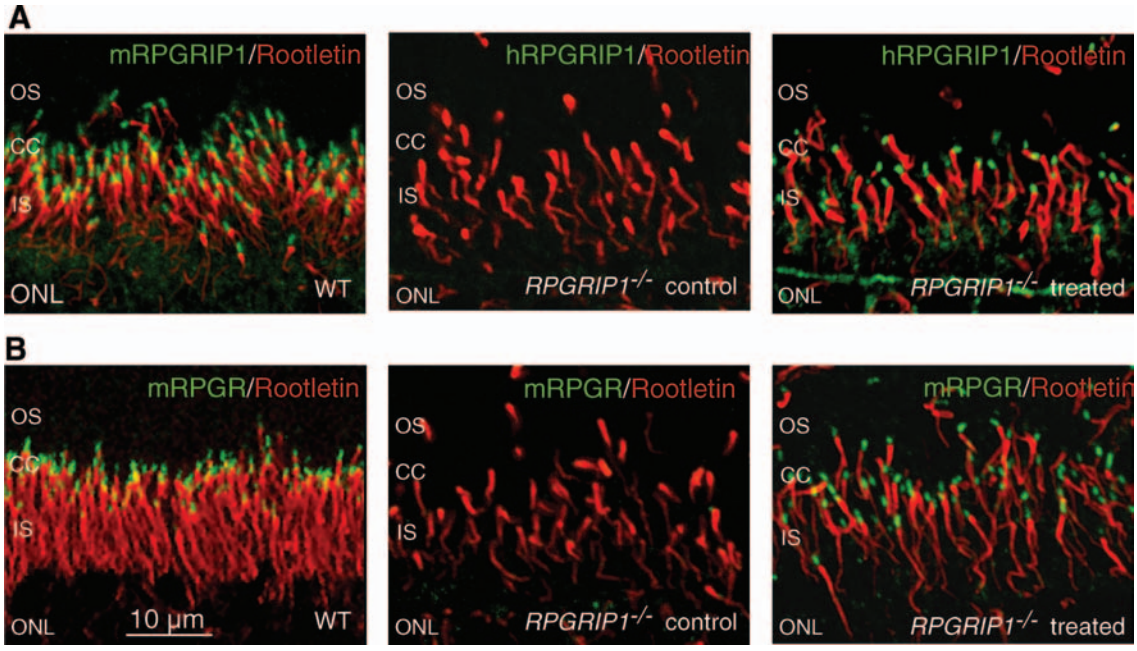

FIG. 2. Subcellular localization of human RPGRIP1 in mouse photoreceptors. (**A**) Human RPGRIP1 expression in an *RPGRIP1*$^{-/-}$ mouse retina after subretinal delivery of the treatment vector. Immunofluorescence staining was performed at 2 weeks after vector delivery. Similar to endogenous mouse RPGRIP1 (green) in WT mouse retina (*left*), human RPGRIP1 (green) correctly localized to the photoreceptor connecting cilium just distal to rootletin (red) in the treated retina (*right*) but not in the control retina (*middle*). (**B**) Expression of human RPGRIP1 led to the return of mouse RPGR (green) at the connecting cilium, also just distal to rootletin (red), in the treated retina (*right*). RPE, retinal pigment epithelium; OS, outer segment; CC, connecting cilium; IS, inner segment; ONL, outer nuclear layer.

age, the treatment effect on cone function persisted, with geometric mean cone ERG b-wave amplitude being 20 and 4 μV for treated and control eyes, respectively ($p < 0.001$). Overall, treatment led to a 200% improvement in rod function and a 400% improvement in cone function as measured by rod and cone ERG b-wave amplitudes at the last time point (5 months).

Longitudinal analysis of the ERG amplitude data from 2 through 5 months of age (includes all data shown in Fig. 3) showed that treatment significantly slowed the course of disease for both rods and cones. As shown in Table 1, the mean rates of monthly decline without treatment were 37% for the rod a-wave, 22% for the rod b-wave, and 25% for the cone b-wave. With treatment, these rates of decline fell to 8% for the rod a-wave and rod b-wave and to no detectable decline for the cone b-wave—in each case a significant slowing of disease course. Representative rod and cone ERGs at 5 months of age are shown in Fig. 6A to illustrate waveforms in treated and control eyes. By 5 months of age, many animals had profoundly reduced rod ERGs and nondetectable cone ERGs in their control eyes. In contrast, their treated eyes still had substantial rod and cone responses at this age, albeit still substantially lower than those of the WT (at approximately one-third of WT level).

Treatment with human RPGRIP1 replacement gene improves photoreceptor morphology and prolongs survival

One of the hallmarks of photoreceptor degeneration in mice lacking RPGRIP1 is severe disruption of the photoreceptor outer segments accompanied by mislocalization of rhodopsin and cone opsin in the cell bodies (Zhao *et al.*, 2003). We performed immunofluorescence staining for rhodopsin and cone opsins on frozen retinal sections from treated and control eyes at approximately 3 months of age. Rhodopsin was found primarily in the rod outer segments of WT photoreceptors (Fig. 4A, left). In the control retina, rod outer segments were severely shortened, and because of rhodopsin mislocalization, the outer and inner segments could not be easily differentiated. There was also obvious ectopic rhodopsin staining in the perinuclear region (Fig. 4A, middle). In the treated retina (Fig. 4A, right), rhodopsin was clearly partitioned to the outer segments, which were longer and appeared better organized than in the control retina. Similarly, compared with the WT (Fig. 4B, left), cone outer segments were severely shortened in the control retina and cone numbers appeared reduced as well (Fig. 4B, middle). In the treated retina (Fig. 4B, right), cone outer segment length and cell density appeared comparable to those of the WT. These data suggest an overall improvement in morphology in the treated retinas compared with the controls.

Photoreceptor morphology was further evaluated by light microscopy at 3 months of age ($n = 3$ pairs of eyes). Both superior and inferior retina along the vertical meridian are shown in Fig. 5A. In the control eye (Fig. 5A, middle panels) at this time point, the outer nuclear layer has been reduced to about 3 or 4 rows of photoreceptor nuclei compared with the 9–11 rows of cells seen in the WT (Fig. 5A, left panels). In addition, photoreceptor outer and inner segments in the control eyes are severely shortened and highly disorganized. In contrast, the treated retinas (Fig. 5A, right panels) showed longer and better

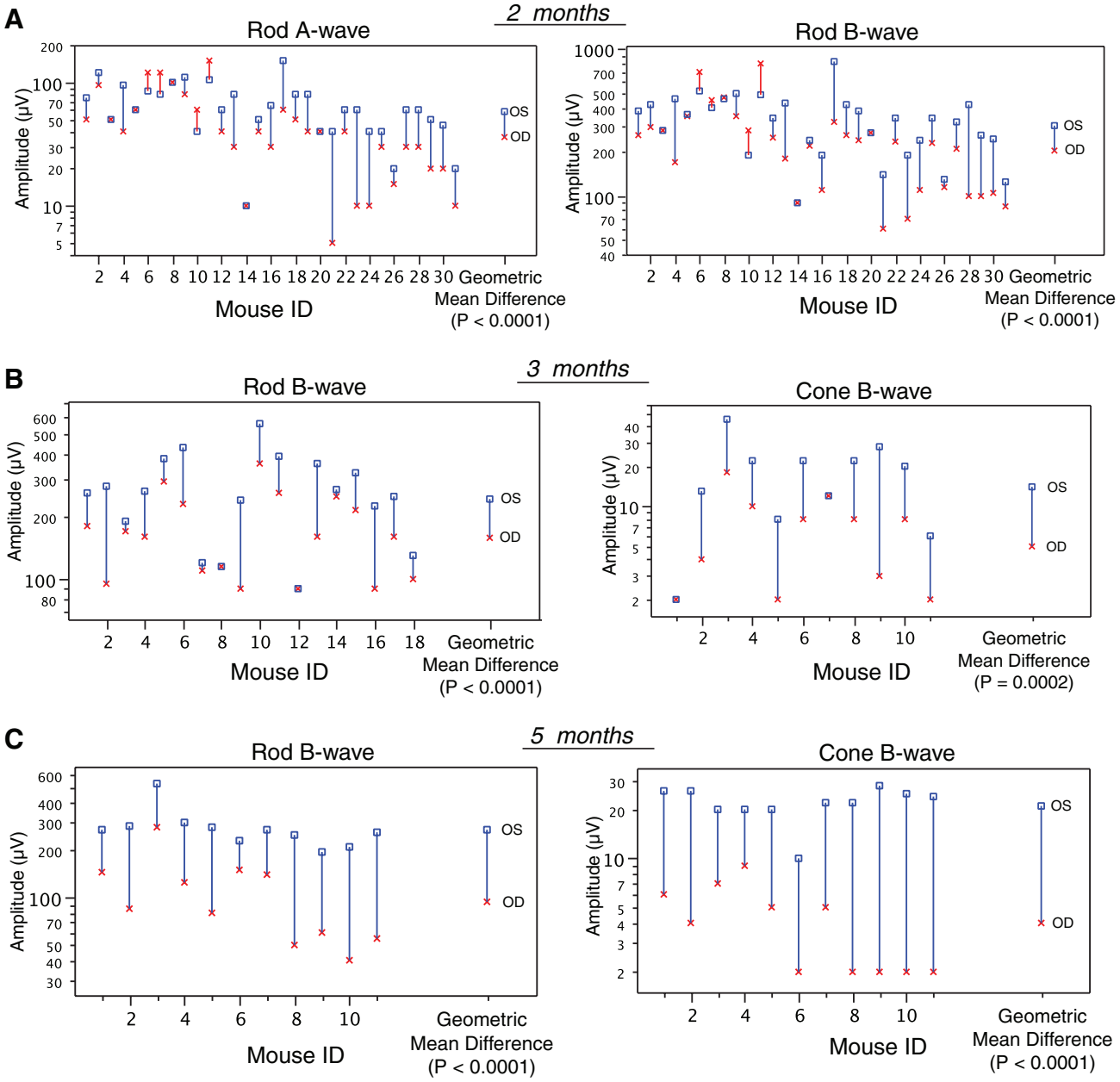

FIG. 3. Preservation of photoreceptor function as measured by rod and cone ERGs. Shown are rod a- and b-wave ERG amplitudes from control and treated eyes at 2 (**A**; $n = 31$), 3 (**B**; $n = 18$), and 5 months of age (**C**; $n = 11$) in the recipient *RPGRIP1*$^{-/-}$ mice. Mice 1–6 in (**A**) and (**B**) represent the same animals tested at the two time points. At the 2-month time point, most mice tested had higher a- and b-wave amplitudes in the treated eyes compared with the control eyes. At the 3- and 5-month time points, all treated eyes had larger responses. The differences between the treated and control eyes were statistically significant at all three time points. Cone ERG b-wave data for treated and control fellow eyes are shown at the 3-month (**B**; $n = 11$) and 5-month (**C**; $n = 11$) time points. The mean cone ERG amplitude was significantly higher in the treated eyes at both time points. Color images available online at www.liebertonline.com/hum.

organized outer segments as well as a thicker outer nuclear layer (six or seven rows). Although markedly improved, the treated retinas did not fully reach the level of retinal morphology observed in WT retina as measured by outer segment length and outer nuclear layer thickness. Figure 5B shows electron microscopy images of treated and control retinas presented in Fig. 5A to further illustrate the well-organized photoreceptor outer segments in the treated eye.

Figure 5C shows morphometric analysis of retinal histology in a representative pair of treated and control eyes. The combined inner/outer segment length and outer nuclear layer thickness were measured at three locations on either side of the optic nerve head along the vertical meridian of the retinal sections. The measurements from three independent locations in each hemisphere were combined and analyzed. The inner/outer segments were significantly longer in the

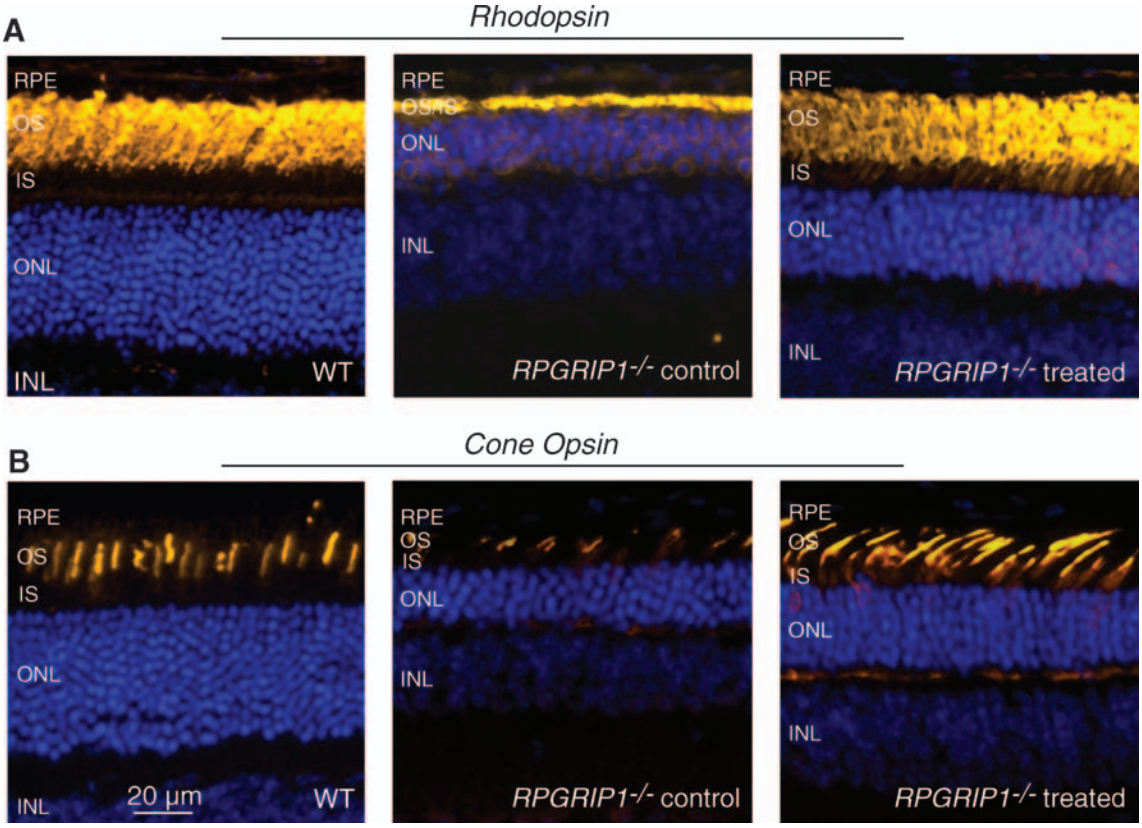

FIG. 4. Immunofluorescence staining (yellow) for rhodopsin (**A**) and cone opsin (**B**) in treated and control *RPGRIP1*$^{-/-}$ mouse retinas at 3 months of age. (**A**) Rhodopsin normally localized in photoreceptor outer segments (WT). In the control *RPGRIP1*$^{-/-}$ retina (*middle*), the inner and outer segments were severely shortened and indistinguishable, and rhodopsin mislocalized to the inner segments and cell bodies. In the treated retina (*right*), rod outer segments were elongated and rhodopsin is largely partitioned to the outer segments with the inner and outer segment layers clearly distinguishable from one another. (**B**) Staining for green cone opsin shows more plentiful cone photoreceptors and with better preserved outer segments in the treated *RPGRIP1*$^{-/-}$ mouse retina compared with the control. Some cone opsin mislocalization was still present in the treated retina compared with the WT. Note also the thicker ONL in the treated retina compared with the control. Sections were counterstained with Hoechst dye 33342 to highlight cell nuclei (blue). The treated retina shown was one with the best rescue from among 10 pairs of eyes analyzed. RPE, retinal pigment epithelium; OS, outer segments; IS, inner segments; ONL, outer nuclear layer; INL, inner nuclear layer.

treated eyes than in the control eyes, with a mean difference of $7.1 \pm 0.38\,\mu$m ($n = 3$ pairs; $p = 0.0028$). The outer nuclear layer was also better preserved in the treated eye than in the control eye, with a $7.3\,\mu\text{m} \pm 0.05$ mean difference ($n = 3$ pairs; $p < 0.0001$). These data demonstrate that significantly more photoreceptors survived in the treated retinas and that the surviving cells maintained better morphology as measured by inner plus outer segment length, a critical indicator of overall photoreceptor cell health. Figure 6B illustrates representative retinal morphology in a pair of treated and control eyes at the final study time point. In the control eyes there were between zero and two rows of photoreceptors remaining at this age, whereas the treated eyes typically retained four or five rows of photoreceptors.

Discussion

Nonmotile or primary cilia are increasingly being appreciated as having a diverse array of important functions. The connecting cilium in photoreceptors, the link between the light-sensing outer segment and biosynthetic inner segment, occupies a position of central importance in photoreceptor cell biology. There are a number of retinal dystrophies and types of Usher syndrome that are caused by genetic defects affecting the connecting cilia. A partial list includes RPGR (X-linked RP), Lebercilin (LCA), and CEP290 (LCA). RPGRIP1 is the first ciliary protein to be addressed in a replacement gene therapy approach, and the results from our study could prove important for the design of gene therapy protocols for other forms of ciliary defects that lead to photoreceptor degeneration. The present study was designed to test the potential therapeutic efficacy of a human-derived *RPGRIP1* replacement gene in a murine model of LCA lacking RPGRIP1. This study is a follow-up to our previous study in which we showed that a *RPGRIP1* replacement gene of murine origin led to improvement in photoreceptor function and survival in *RPGRIP1*$^{-/-}$ mice (Pawlyk *et al.*, 2005). In the previous study, we used a promoter derived from the mouse rhodopsin gene that drove expression primarily in rod photoreceptor cells. As a result the rescue was limited to rod photoreceptors. For human gene therapy, it is imperative that the replacement gene be derived from the

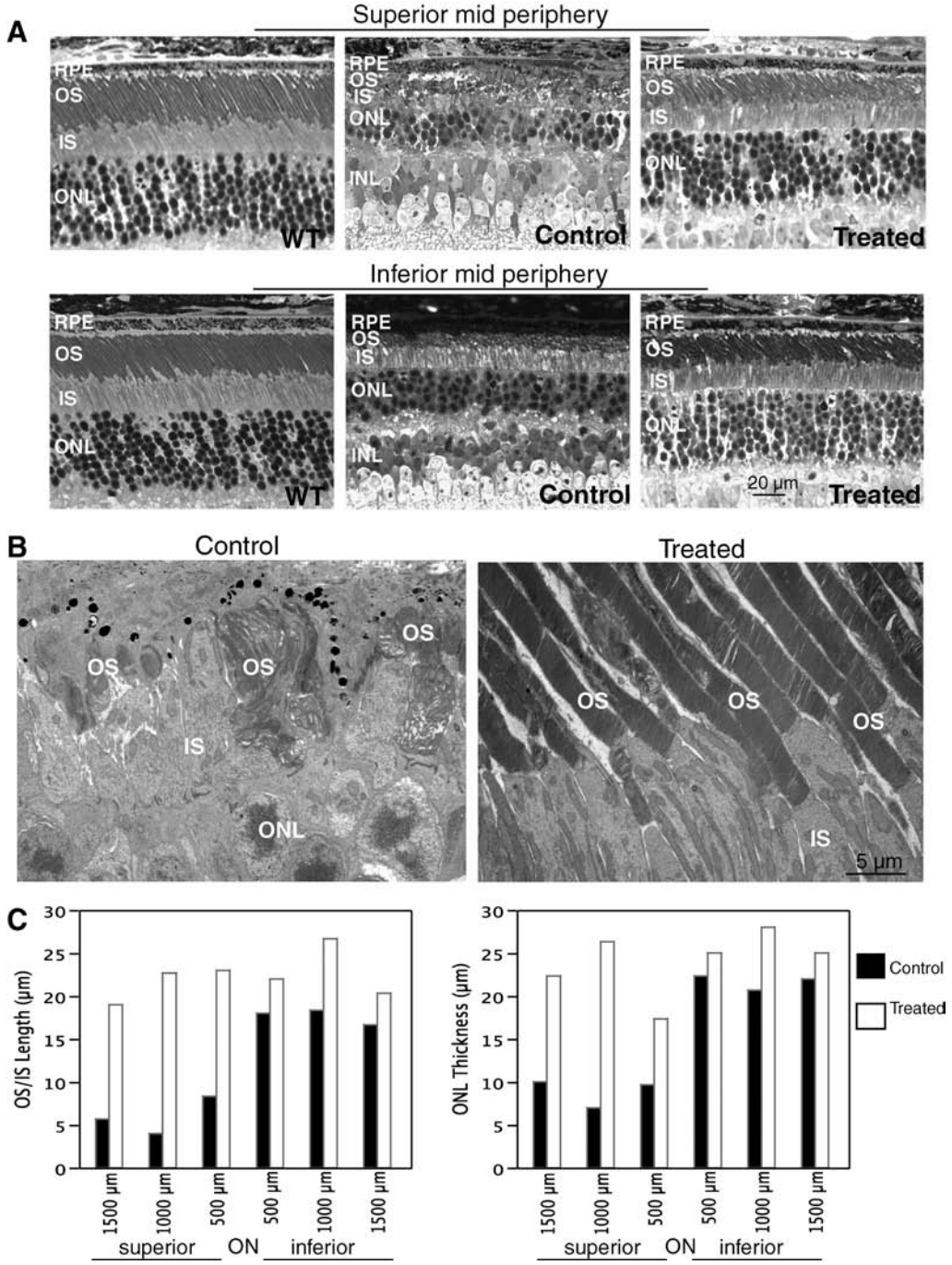

FIG. 5. Morphological analyses of treated and control *RPGRIP1*$^{-/-}$ mouse retinas at 3 months of age. (**A**) Light micrographs of the midperipheral region in the superior and inferior retinal hemispheres. In both hemispheres the control retina has approximately three or four rows of remaining cells in the ONL with shortened and disorganized photoreceptor inner and outer segments. In contrast, the treated eye has six or seven rows of cells in the ONL with well-organized and longer inner and outer segments in both hemispheres. A WT retina is shown for comparison. (**B**) Electron micrographs of the treated and control retinas shown in (**A**). The treated retina retained well-organized outer segment disc structures. (**C**) Variable rescue of photoreceptor cells in different regions of the *RPGRIP1*$^{-/-}$ treated retina. Shown are morphometric measurements of outer nuclear layer thickness (*left*) and combined inner and outer segment lengths (*right*) along the vertical meridian in a representative pair of treated and control retinas (ON, optic nerve). RPE, retinal pigment epithelium; OS, outer segments; IS, inner segments; ONL, outer nuclear layer; INL, inner nuclear layer.

human genome, and, in the case of *RPGRIP1*, its expression needs to target both rods and cones. We have established that a promoter derived from the human rhodopsin kinase gene drives transgene expression in both rods and cones (Young *et al.*, 2003; Khani *et al.*, 2007; Sun *et al.*, 2010). The relatively small size of the RK promoter (~200 bp) is ideal for use in combination with the *RPGRIP1* replacement gene because the latter is relatively large (~4 kb), approaching the packaging size limit of AAV vectors. This short RK promoter was incorporated into our replacement gene design to drive

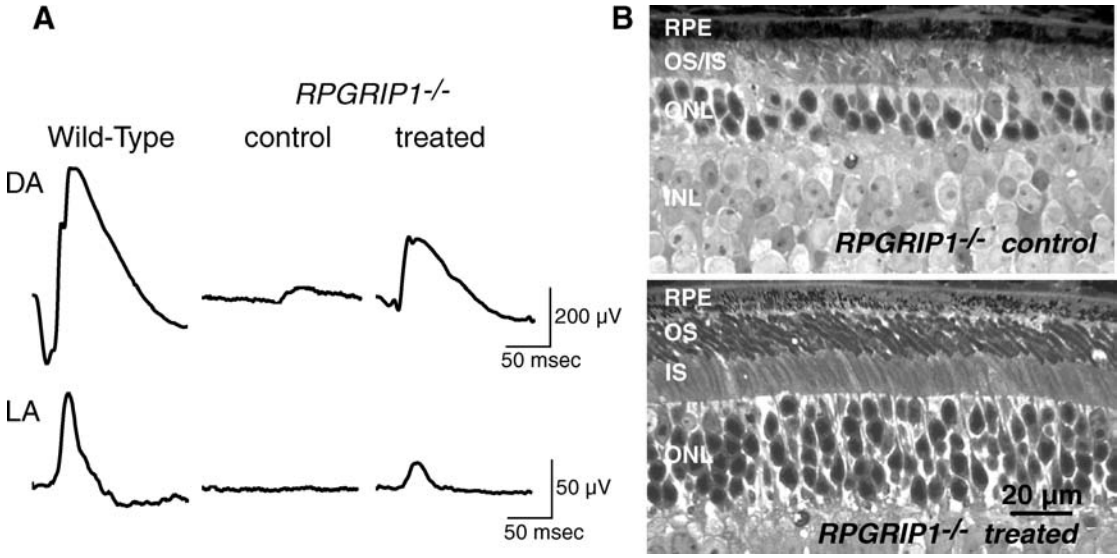

FIG. 6. (**A**) Representative dark-adapted (DA) and light-adapted (LA) ERG waveforms from a pair of treated and control *RPGRIP1*$^{-/-}$ eyes at 5 months of age. WT ERG waveforms are shown for comparison. The control eye has a profoundly reduced rod ERG and a nondetectable cone ERG at this age. The treated eye, however, has substantial rod and cone ERGs at this time point that are approximately one-third of WT values. (**B**) Representative light photomicrographs of the superior retina from the same pair of *RPGRIP1*$^{-/-}$ eyes shown in (**A**). The control eye has only about two rows of photoreceptor cells remaining in the ONL at this age, with severely shortened and disorganized inner/outer segments. In contrast, the treated eye has retained up to five rows of photoreceptor cells with longer and organized inner/outer segments.

a human *RPGRIP1* replacement gene. A further technical difference from the previous study is that we chose to package the therapeutic gene construct into AAV2/8 to take advantage of the known benefits of this version of AAV vector, such as faster onset of transgene expression and higher expression levels in photoreceptor cells (G.S. Yang *et al.*, 2002; Allocca *et al.*, 2007; Natkunarajah *et al.*, 2008). The AAV2/8 vector proved successful in driving rapid expression because we could detect human RPGRIP1 protein by immunofluorescence as early as 1 week postinjection. These data represent a marked improvement over a prior unpublished study of similar design and scope, in which we packaged the replacement gene in an AAV2/5 vector. Human RPGRIP1 expression from the AAV2/5 vector in recipient mice was lower than what was found in the present study, and the therapeutic efficacy appeared minimal (our unpublished data).

The human RPGRIP1 protein expressed from the replacement gene was identical in apparent molecular weight to that of the native RPGRIP1 from human donor retinal tissues. The human RPGRIP1 is predicted to have a molecular mass of 147 kDa, and the major mouse RPGRIP1 variant is predicted to have a molecular mass of 152 kDa. These are considerably smaller than the values (170 and 190 kDa) that we estimated on the basis of motility in sodium dodecyl sulfate (SDS)–polyacrylamide gels. We believe these differences can be reasonably explained by the high content of negatively charged amino acid resides (glutamic acid) in these proteins, especially in mouse RPGRIP1. A higher acidic residue content is known to retard motility of the polypeptides on SDS–polyacrylamide gels, thus giving higher apparent molecular weight estimates (Graceffa *et al.*, 1992; Korschen *et al.*, 1995; Iakoucheva *et al.*, 2001). For example, the RPGR protein exhibits a similar behavior because of high glutamic acid content, having a much higher apparent molecular weight than would be predicated from its sequence. We conclude that the human RPGRIP1 coding sequence used in the replacement gene construct is indeed the same form that is expressed endogenously in human photoreceptors.

The expression level of human RPGRIP1 protein in recipient mouse retinas appeared lower than that of endogenous RPGRIP1 from WT mouse retinas. The reason for the lower expression is not fully understood at this time. We do not believe this is related to the strength of the RK promoter because expression levels from the transgenes were all quite high in at least four other constructs using this promoter. One explanation is that the inner retinal cells from the WT and human retinas also contributed to the total RPGRIP1 content on immunoblots, which would result in an underestimate of the expression level in the treated retinas. This possibility can be clarified in future experiments. Other explanations may be a reduced stability of human RPGRIP1 transcript, a shorter half-life of human RPGRIP1 protein, or difficulty in human RPGRIP1 protein folding in a mouse photoreceptor milieu. If the last hypothesis is correct, one would expect that this same vector should yield a higher expression level in recipient human photoreceptors in a clinical application. Even if the transgene expression level remains less than the endogenous level, we do not believe that poses a significant barrier to early clinical studies. The RK promoter exhibited excellent tissue specificity; we have not observed ectopic expression in RPE, inner retina, or nonocular tissues. Nor have we observed any apparent pathology or increased mortality in mice that received vector injections.

Human RPGRIP1 protein is functional in mouse photoreceptors as demonstrated both by protein localization

studies and by better photoreceptor function (ERG) and morphology after treatment. Differences were seen in both the quality and numbers of rods and cones between the control and treated eyes. There was an improvement in rhodopsin and cone opsin localization patterns in the treated retinas. Treatment significantly promoted photoreceptor survival and improved photoreceptor morphology in terms of inner/outer segment length and organization, which are important indicators of photoreceptor general health. Retinal function was also greatly improved by treatment. Treated eyes had significantly larger rod and cone ERG amplitudes at all time points tested, and the rate of ERG decline was markedly slowed. These data confirm a therapeutic efficacy for this replacement gene construct in mouse photoreceptors and establish a prototype design for future clinical application in LCA patients with RPGRIP1 deficiency.

Despite marked improvement in retinal function and morphology, rescue of the retinal disease phenotype was not complete. By comparison with WT mice, treated *RPGRIP1*$^{-/-}$ mouse eyes had rod and cone ERG amplitudes that were on average only approximately one-third of WT mouse values at the end point of the study (5 months). It should be noted, however, that subretinal injections in mice can acutely reduce ERG amplitude by as much as 50% (our unpublished observation). Therefore damage associated with subretinal injection could, in part, contribute to the incomplete rescue in the treated eyes. On the other hand, the data show that retinal function continued to decline over time in the treated eyes, as if the treatment did not fully reconstitute RPGRIP1 function in the recipient retinas. We could think of two main reasons to account for this. First, the expression level of transgenic human RPGRIP1 is substantially lower than that of endogenous RPGRIP1 in mice. Second, there is substantial divergence between human and mouse RGPRIP1 sequences, with some regions of the protein bearing no homology between the two species. This is in sharp contrast to the typically high degree of conservation between the two species for many other photoreceptor-specific proteins (e.g., those involved in the phototransduction cascade). Either of these reasons could have accounted for the incomplete rescue observed in this study. Yet another possibility is the existence of RPGRIP1 variants (Castagnet *et al.*, 2003; Lu and Ferreira, 2005; Won *et al.*, 2009). It remains unclear if and to what extent these variants are functionally significant in photoreceptors. The reported variants represent variant portions of the N-terminal RPGRIP1 and do not contain the RPGR-interacting domain located at the C terminus. Therefore, they are not expected to participate in the core function of RPGRIP1, that is, to anchor RPGR in the connecting cilia. Further studies may be necessary to examine the individual roles of the variants in photoreceptor maintenance and function. Given the available data, it is reasonable to predict that the human *RPGRIP1* replacement gene may produce a more favorable outcome in the human photoreceptor environment than in the murine photoreceptor environment.

The results from this study could pave the way for a future clinical trial targeting LCA caused by RPGRIP1 functional deficiency. The rapid disease progression in LCA presents a significant challenge to gene therapy because retention of sufficient photoreceptors in the retina is a prerequisite for a satisfactory therapeutic outcome. In this regard, it is encouraging that LCA associated with *RPGRIP1* gene mutations has been reported by some to present with a more stable and somewhat nonprogressive disease course after the initial rapid decline in visual function (Hanein *et al.*, 2004). Photoreceptors in the central retina appear to persist for long periods of time after visual function becomes unmeasurable (Jacobson *et al.*, 2007). In our own clinic, we have also found by optical coherence tomography that patients with LCA due to *RPGRIP1* mutations can retain a substantial number of photoreceptors even when visual function has largely been lost as measured by visual field and ERGs (our unpublished observations). These clinical observations highlight the potential for treatment in patients who carry *RPGRIP1* gene mutations.

Acknowledgments

The authors thank Dr. Jeng-Shin Lee at the Research Vector Core of Harvard Medical School for AAV vector packaging, the National Disease Research Interchange for providing human retinal tissue, and Norman Michaud for select tissue processing for light microscopy. This work was supported by National Eye Institute grant EY10581, an NEI core grant for Vision Research (P30EY14104), the Foundation Fighting Blindness, the Foundation for Retina Research, and the Massachusetts Lions Eye Research Fund.

Author Disclosure Statement

No competing financial interests exist for any of the authors.

References

Acland, G.M., Aguirre, G.D., Ray, J., Zhang, Q., Aleman, T.S., Cideciyan, A.V., Pearce-Kelling, S.E., Anand, V., Zeng, Y., Maguire, A.M., Jacobson, S.G., Hauswirth, W.W., and Bennett, J. (2001). Gene therapy restores vision in a canine model of childhood blindness. Nat. Genet. 28, 92–95.

Allocca, M., Mussolino, C., Garcia-Hoyos, M., Sanges, D., Iodice, C., Petrillo, M., Vandenberghe, L.H., Wilson, J.M., Marigo, V., Surace, E.M., and Auricchio, A. (2007). Novel adeno-associated virus serotypes efficiently transduce murine photoreceptors. J. Virol. 81, 11372–11380.

Bainbridge, J.W., Smith, A.J., Barker, S.S., Robbie, S., Henderson, R., Balaggan, K., Viswanathan, A., Holder, G.E., Stockman, A., Tyler, N., Petersen-Jones, S., Bhattacharya, S.S., Thrasher, A.J., Fitzke, F.W., Carter, B.J., Rubin, G.S., Moore, A.T., and Ali, R.R. (2008). Effect of gene therapy on visual function in Leber's congenital amaurosis. N. Engl. J. Med. 358, 2231–2239.

Berson, E.L. (1993). Retinitis pigmentosa: the Friedenwald Lecture. Invest. Ophthalmol. Vis. Sci. 34, 1659–1676.

Berson, E.L., Rosner, B., Weigel-DiFranco, C., Dryja, T.P., and Sandberg, M.A. (2002). Disease progression in patients with dominant retinitis pigmentosa and rhodopsin mutations. Invest. Ophthalmol. Vis. Sci. 43, 3027–3036.

Boylan, J.P., and Wright, A.F. (2000). Identification of a novel protein interacting with RPGR. Hum. Mol. Genet. 9, 2085–2093.

Castagnet, P., Mavlyutov, T., Cai, Y., Zhong, F., and Ferreira, P. (2003). RPGRIP1s with distinct neuronal localization and biochemical properties associate selectively with RanBP2 in amacrine neurons. Hum. Mol. Genet. 12, 1847–1863.

Clarke, G., Collins, R.A., Leavitt, B.R., Andrews, D.F., Hayden, M.R., Lumsden, C.J., and McInnes, R.R. (2000). A one-hit model of cell death in inherited neuronal degenerations. Nature 406, 195–199.

Dejneka, N.S., Surace, E.M., Aleman, T.S., Cideciyan, A.V., Lyubarsky, A., Savchenko, A., Redmond, T.M., Tang, W., Wei, Z., Rex, T.S., Glover E, Maguire AM, Pugh, E.N., Jr., Jacobson, S.G., and Bennett, J. (2004). *In utero* gene therapy rescues vision in a murine model of congenital blindness. Mol. Ther. 9, 182–188.

den Hollander, A.I., Roepman, R., Koenekoop, R.K., and Cremers, F.P. (2008). Leber congenital amaurosis: Genes, proteins and disease mechanisms. Prog. Retin. Eye Res. 27, 391–419.

Dryja, T.P., Adams, S.M., Grimsby, J.L., McGee, T.L., Hong, D.H., Li, T., Andreasson, S., and Berson, E.L. (2001). Null RPGRIP1 alleles in patients with Leber congenital amaurosis. Am J. Hum. Genet. 68, 1295–1298.

Flannery, J.G., Zolotukhin, S., Vaquero, M.I., LaVail, M.M., Muzyczka, N., and Hauswirth, W.W. (1997). Efficient photoreceptor-targeted gene expression *in vivo* by recombinant adeno-associated virus. Proc. Natl. Acad. Sci. U.S.A. 94, 6916–6921.

Fulton, A.B., Hansen, R.M., and Mayer, D.L. (1996). Vision in Leber congenital amaurosis. Arch. Ophthalmol. 114, 698–703.

Gerber, S., Perrault, I., Hanein, S., Barbet, F., Ducroq, D., Ghazi, I., Martin-Coignard, D., Leowski, C., Homfray, T., Dufier, J.L., Munnich, A., Kaplan, J., and Rozet, J.M. (2001). Complete exon–intron structure of the RPGR-interacting protein (RPGRIP1) gene allows the identification of mutations underlying Leber congenital amaurosis. Eur. J. Hum. Genet. 9, 561–571.

Graceffa, P., Jancso, A., and Mabuchi, K. (1992). Modification of acidic residues normalizes sodium dodecyl sulfate–polyacrylamide gel electrophoresis of caldesmon and other proteins that migrate anomalously. Arch. Biochem. Biophys. 297, 46–51.

Hanein, S., Perrault, I., Gerber, S., Tanguy, G., Barbet, F., Ducroq, D., Calvas, P., Dollfus, H., Hamel, C., Lopponen, T., Munier, F., Santos, L., Shalev, S., Zafeiriou, D., Dufier, J.L., Munnich, A., Rozet, J.M., and Kaplan, J. (2004). Leber congenital amaurosis: Comprehensive survey of the genetic heterogeneity, refinement of the clinical definition, and genotype–phenotype correlations as a strategy for molecular diagnosis. Hum. Mutat. 23, 306–317.

Hauswirth, W.W., Aleman, T.S., Kaushal, S., Cideciyan, A.V., Schwartz, S.B., Wang, L., Conlon, T.J., Boye, S.L., Flotte, T.R., Byrne, B.J., and Jacobson, S.G. (2008). Treatment of leber congenital amaurosis due to RPE65 mutations by ocular subretinal injection of adeno-associated virus gene vector: Short-term results of a phase I trial. Hum. Gene Ther. 19, 979–990.

Heher, K.L., Traboulsi, E.I., and Maumenee, I.H. (1992). The natural history of Leber's congenital amaurosis: Age-related findings in 35 patients. Ophthalmology 99, 241–245.

Hong, D.H., Yue, G., Adamian, M., and Li, T. (2001). Retinitis pigmentosa GTPase regulator (RPGR)-interacting protein is stably associated with the photoreceptor ciliary axoneme and anchors RPGR to the connecting cilium. J. Biol. Chem. 276, 12091–12099.

Iakoucheva, L.M., Kimzey, A.L., Masselon, C.D., Smith, R.D., Dunker, A.K., and Ackerman, E.J. (2001). Aberrant mobility phenomena of the DNA repair protein XPA. Protein Sci. 10, 1353–1362.

Jacobson, S.G., Cideciyan, A.V., Aleman, T.S., Sumaroka, A., Schwartz, S.B., Roman, A.J., and Stone, E.M. (2007). Leber congenital amaurosis caused by an RPGRIP1 mutation shows treatment potential. Ophthalmology 114, 895–898.

Khani, S.C., Pawlyk, B.S., Bulgakov, O.V., Kasperek, E., Young, J.E., Adamian, M., Sun, X., Smith, A.J., Ali, R.R., and Li, T. (2007). AAV-mediated expression targeting of rod and cone photoreceptors with a human rhodopsin kinase promoter. Invest. Ophthalmol. Vis. Sci. 48, 3954–3961.

Koenekoop, R.K. (2004). An overview of Leber congenital amaurosis: A model to understand human retinal development. Surv. Ophthalmol. 49, 379–398.

Koenekoop, R.K. (2005). RPGRIP1 is mutated in Leber congenital amaurosis: A mini-review. Ophthalmic Genet. 26, 175–179.

Korschen, H.G., Illing, M., Seifert, R., Sesti, F., Williams, A., Gotzes, S., Colville, C., Muller, F., Dose, A., Godde, M., Molday, L., Kaupp, U.B., and Molday, R.S. (1995). A 240 kDa protein represents the complete β subunit of the cyclic nucleotide-gated channel from rod photoreceptor. Neuron 15, 627–636.

Lu, X., and Ferreira, P.A. (2005). Identification of novel murine- and human-specific RPGRIP1 splice variants with distinct expression profiles and subcellular localization. Invest. Ophthalmol. Vis. Sci. 46, 1882–1890.

Maguire, A.M., Simonelli, F., Pierce, E.A., Pugh, E.N., Jr., Mingozzi, F., Bennicelli, J., Banfi, S., Marshall, K.A., Testa, F., Surace, E.M., Rossi, S., Lyubarsky, A., Arruda, V.R., Konkle, B., Stone, E., Sun, J., Jacobs, J., Dell'Osso, L., Hertle, R., Ma, J.X., Redmond, T.M., Zhu, X., Hauck, B., Zelenaia, O., Shindler, K.S., Maguire, M.G., Wright, J.F., Volpe, N.J., McDonnell, J.W., Auricchio, A., High, K.A., and Bennett, J. (2008). Safety and efficacy of gene transfer for Leber's congenital amaurosis. N. Engl. J. Med. 358, 2240–2248.

Molday, R. (1988). Monoclonal antibodies to rhodopsin and other proteins of rod outer segments. In: Osborne, N., and Chader, G., eds. *Progress in Retinal Research* (Pergamon Press, New York), *pp.* 173–209.

Narfstrom, K., Katz, M.L., Bragadottir, R., Seeliger, M., Boulanger, A., Redmond, T.M., Caro, L., Lai, C.M., and Rakoczy, P.E. (2003). Functional and structural recovery of the retina after gene therapy in the RPE65 null mutation dog. Invest. Ophthalmol. Vis. Sci. 44, 1663–1672.

Natkunarajah, M., Trittibach, P., McIntosh, J., Duran, Y., Barker, S.E., Smith, A.J., Nathwani, A.C., and Ali, R.R. (2008). Assessment of ocular transduction using single-stranded and self-complementary recombinant adeno-associated virus serotype 2/8. Gene Ther. 15, 463–467.

Pang, J.J., Chang, B., Kumar, A., Nusinowitz, S., Noorwez, S.M., Li, J., Rani, A., Foster, T.C., Chiodo, V.A., Doyle, T., Li, H., Malhotra, R., Teusner, J.T., McDowell, J.H., Min, S.H., Li, Q., Kaushal, S., and Hauswirth, W.W. (2006). Gene therapy restores vision-dependent behavior as well as retinal structure and function in a mouse model of RPE65 Leber congenital amaurosis. Mol. Ther. 13, 565–572.

Pawlyk, B.S., Smith, A.J., Buch, P.K., Adamian, M., Hong, D.H., Sandberg, M.A., Ali, R.R., and Li, T. (2005). Gene replacement therapy rescues photoreceptor degeneration in a murine model of Leber congenital amaurosis lacking RPGRIP. Invest. Ophthalmol. Vis. Sci. 46, 3039–3045.

Roepman, R., Bernoud-Hubac, N., Schick, D.E., Maugeri, A., Berger, W., Ropers, H.-H., Cremers, F.P.M., and Ferreira, P.A. (2000). The retinitis pigmentosa GTPase regulator (RPGR) interacts with novel transport-like proteins in the outer segments of rod photoreceptors. Hum. Mol. Genet. 9, 2095–2105.

Sun, X., Pawlyk, B., Xu, X., Liu, X., Bulgakov, O.V., and Adamian, M. (2010). Gene therapy with a promoter targeting both rods and cones rescues retinal degeneration caused by AIPL1 mutations. Gene Ther. 17, 117–131.

Tan, M.H., Smith, A.J., Pawlyk, B., Xu, X., Liu, X., Bainbridge, J.B., Basche, M., McIntosh, J., Tran, H.V., Nathwani, A., and

Ali, R.R. (2009). Gene therapy for retinitis pigmentosa and Leber congenital amaurosis caused by defects in AIPL1: Effective rescue of mouse models of partial and complete Aipl1 deficiency using AAV2/2 and AAV2/8 vectors. Hum. Mol. Genet. 18, 2099–2114.

Vervoort, R., Lennon, A., Bird, A.C., Tulloch, B., Axton, R., Miano, M.G., Meindl, A., Meitinger, T., Ciccodicola, A., and Wright, A.F. (2000). Mutational hot spot within a new RPGR exon in X-linked retinitis pigmentosa. Nat. Genet. 25, 462–466.

Wang, H., den Hollander, A.I., Moayedi, Y., Abulimiti, A., Li, Y., Collin, R.W., Hoyng, C.B., Lopez, I., Bray, M., Lewis, R.A., Lupski, J.R., Mardon, G., Koenekoop, R.K., and Chen, R. (2009). Mutations in SPATA7 cause Leber congenital amaurosis and juvenile retinitis pigmentosa. Am. J. Hum. Genet. 84, 380–387.

Won, J., Gifford, E., Smith, R.S., Yi, H., Ferreira, P.A., Hicks, W.L., Li, T., Naggert, J.K., and Nishina, P.M. (2009). RPGRIP1 is essential for normal rod photoreceptor outer segment elaboration and morphogenesis. Hum. Mol. Genet. 18, 4329–4339.

Xiao, X., Li, J., and Samulski, R.J. (1998). Production of high-titer recombinant adeno-associated virus vectors in the absence of helper adenovirus. J. Virol. 72, 2224–2232.

Yang, G.S., Schmidt, M., Yan, Z., Lindbloom, J.D., Harding, T.C., Donahue, B.A., Engelhardt, J.F., Kotin, R., and Davidson, B.L. (2002). Virus-mediated transduction of murine retina with adeno-associated virus: effects of viral capsid and genome size. J. Virol. 76, 7651–7660.

Yang, J., Liu, X., Yue, G., Adamian, M., Bulgakov, O., and Li, T. (2002). Rootletin, a novel coiled-coil protein, is a structural component of the ciliary rootlet. J. Cell. Biol. 159, 431–440.

Young, J.E., Vogt, T., Gross, K.W., and Khani, S.C. (2003). A short, highly active photoreceptor-specific enhancer/promoter region upstream of the human rhodopsin kinase gene. Invest. Ophthalmol. Vis. Sci. 44, 4076–4085.

Zhao, Y., Hong, D.H., Pawlyk, B., Yue, G., Adamian, M., Grynberg, M., Godzik, A., and Li, T. (2003). The retinitis pigmentosa GTPase regulator (RPGR)-interacting protein: Subserving RPGR function and participating in disk morphogenesis. Proc. Natl. Acad. Sci. U.S.A. 100, 3965–3970.

Address correspondence to:
Dr. Tiansen Li
National Eye Institute
Bethesda, MD 20892

E-mail: Tiansen.Li@nih.gov

Received for publication December 9, 2009;
accepted after revision April 12, 2010.

Published online: July 16, 2010.